Relativistic collisional current-filamentation instability and two-stream instability in dense plasma

Biao Hao,[1] Z.-M. Sheng,[1,2,*] C. Ren,[3,4,5] and J. Zhang[1,2]
[1]*Beijing National Laboratory of Condensed Matter Physics, Institute of Physics, CAS, Beijing 100190, China*
[2]*Department of Physics, Shanghai Jiao Tong University, Shanghai 200240, China*
[3]*Department of Mechanical Engineering, University of Rochester, Rochester, New York 14623, USA*
[4]*Department of Physics and Astronomy, University of Rochester, Rochester, New York 14623, USA*
[5]*Laboratory for Laser Energetics, University of Rochester, Rochester, New York 14623, USA*
(Received 6 January 2009; published 27 April 2009)

The collisional effects on the current-filamentation instability (CFI) and the two-stream instability (TSI), which appear as a relativistic intense electron beam penetrating into a cold dense plasma, are investigated. It is shown that the growth rate of the CFI mode is first attenuated and then enhanced by the collisional effects as the density ratio of the background plasma to the beam increases. Meanwhile, the maximum CFI growth rate is shifted to the long-wavelength region due to both the bulk plasma density increase and the collisional effects, resulting in larger filaments formation. On the other hand, collisional effects mainly attenuate the TSI and finally stabilize it. Numerical solutions under parameters close to the fast ignition scenario (FIS) are given, which show that the CFI growth rate can be enhanced by 2 orders of magnitude instead of being suppressed in the dense region. Therefore, the CFI-induced electron filaments formation and the resultant kinetic anomalous heating are potentially significant for the target heating in the FIS.

DOI: 10.1103/PhysRevE.79.046409 PACS number(s): 52.35.Qz, 52.20.Fs, 52.50.Gj, 52.57.Kk

I. INTRODUCTION

Beam-plasma interaction and the associated current-filamentation instability (CFI), two-stream instability (TSI), and the coupled two-stream-filamentation instability, which can result in strong magnetic fields [1] and kinetic anomalous heating [2–6], are significantly important for the transport and energy deposition of a large flux of relativistic electron beam penetrating a plasma. In a dense cold bulk plasma, in particular, collisions between the bulk plasma particles can obviously alter these instabilities. Thus they have attracted renewed attentions recently [6–12] because they are closely related to the fast ignition scenario (FIS) of laser inertial confinement fusion [13]. Although it is shown in the collisionless case that the fastest growing branch is the coupled two-stream-filamentation mode [14,15], our recent investigations show that the filamentation mode may grow faster than the coupled mode in the collisional case [16] when the density ratio of the bulk plasma to the beam gets over 60 under the same parameters of the present paper. Therefore the electromagnetic CFI appears to be the primary instability in the FIS, which we will mainly focus on here. For comparison we also include the collisional electrostatic TSI in the present paper.

There have been a number of investigations on the collisional CFI ever since 1970s. But right from the beginning, incompatible results have been obtained, showing that collisional effects sometimes enhance the CFI [11,12,17–19] while sometimes attenuate and stabilize it [8,9,20]. The detailed process remained unclear for a long time. Recently we gave a generalized kinetic theory on the nonrelativistic CFI in a collisional plasma [10], which clarifies that collisional effects can in fact play dual roles. On one hand, collisions cause detuning between the particle density perturbations and the reactive fields, which attenuate the CFI. On the other hand, they interfere with the collective motion and cancel the stabilization effect of the dense plasma, which enhance the CFI. Finally the combination tends to attenuate the CFI for a symmetric (where the bulk electron density equals the beam density) or quasisymmetric counterstreaming system while enhancing it for an extremely asymmetric (where the bulk electron density is much larger than the beam density) counterstreaming system. The enhancement can be very significant for an extremely dense plasma.

In the present work we extend our previous studies to the relativistic case and mainly focus on the situation close to the cone guided FIS [21]. Although a complete study should include the space-charge effect [22], our recent investigations show that collisional effects can indeed greatly decrease it. This is to be argued in another paper so we do not consider it here. Under such confinement the present investigation shows that collisional effects cannot stabilize but enhance the CFI in the dense region. Meanwhile, the fastest growing CFI mode is shifted to the long-wavelength region, resulting in much larger filaments, which is essential for the evolution and coalescence of the filaments [23,24]. Unlike the previous investigations [9–11] finding that the electromagnetic filamentation mode could have a real frequency part, our present study which uses the most accurate Padé approximation Z_{53} given in [25] for the plasma dispersion function discloses that the filamentation mode is always purely growing. Therefore, there should be no Landau damping [26] for the CFI as we once claimed in our previous study [10].

For comparison we also study the collisional effects on the TSI analytically. Previous analytical investigation [27] showed that collisional effects can also either enhance or

*zmsheng@aphy.iphy.ac.cn

attenuate the TSI, while the recent studies [7,11] related to the FIS show that the TSI is attenuated. Different from the previous studies [11,27], here we treat both the beam and the background plasma kinetically and focus on the physical process. Our calculation shows that the TSI is fully stabilized when the background plasma reaches the solid density. This is in good agreement with the collisional particle-in-cell simulation [7].

The paper is organized as follows. In Sec. II, the basic theory for the linear collisional dispersion relation is presented. In Sec. III, the collisional dispersion equation is solved. Numerical results relevant to the FIS for the CFI and the TSI are given in Secs. III A and III B, respectively. The involved physical mechanisms are clarified in details. Finally, we conclude in Sec. IV.

II. KINETIC DISPERSION RELATION

We start with a homogeneous, spatially infinite, and unmagnetized plasma, where the ions are deuterium or tritium immobile to form a charge neutralized background. The system is described by the Vlasov-Krook-Maxwell equations[18,28,29];

$$\frac{\partial f_\alpha}{\partial t} + \vec{v}_\alpha \cdot \frac{\partial f_\alpha}{\partial \vec{r}} + q_\alpha \left(\vec{E} + \frac{\vec{v}_\alpha \times \vec{B}}{c} \right) \cdot \frac{\partial f_\alpha}{\partial \vec{p}_\alpha} = \nu_\alpha (f_{0\alpha} - f_\alpha), \tag{1}$$

$$\vec{\nabla} \times \vec{B} = \frac{1}{c}\frac{\partial \vec{E}}{\partial t} + \frac{4\pi}{c}\sum_\alpha \vec{j}_\alpha, \tag{2}$$

$$\vec{\nabla} \times \vec{E} = -\frac{1}{c}\frac{\partial \vec{B}}{\partial t}, \tag{3}$$

where $\alpha = b, p$ label the beam electrons and the background electrons, respectively, $\vec{j}_\alpha = q_\alpha n_\alpha \vec{v}_\alpha$, and q_α, n_α, ν_α, and $f_{0\alpha}$ correspond to the electron charge, the electron density, the effective collision frequency, and the equilibrium distribution function, respectively. Although the Krook model does not conserve the particle number, momentum, and energy, it enables one to obtain analytic results. In this work, all the numerical calculations are constrained to the weak collision case, where the collision frequency is ~ 0.01 (normalized to the background plasma frequency ω_p). This does not only make the Krook model an appropriate approach but also it ensures the assumption of zero-order fields in the linear theory reasonable.

Assume the rigorous current neutralization condition [30] $n_b v_{db} + n_p v_{dp} = 0$ and follow the usual linearizing steps, we can get the general dispersion equation

$$\det \left| \frac{\omega^2}{c^2}\varepsilon_{ij} + k_i k_j - k^2 \delta_{ij} \right| = 0, \tag{4}$$

where the dielectric tensor is

$$\varepsilon_{ij} = \delta_{ij} + \sum_\alpha \frac{\omega_{p\alpha}^2}{n_\alpha \omega^2} \int \frac{p_{\alpha i}}{\gamma_\alpha^*} \frac{\partial f_{0\alpha}}{\partial p_{\alpha j}} \frac{(m_\alpha \gamma_\alpha^* \omega - \vec{k}\cdot\vec{p}_\alpha) d^3\vec{p}_\alpha}{m_\alpha \gamma_\alpha^* (\omega + i\nu_\alpha) - \vec{k}\cdot\vec{p}_\alpha} + \sum_\alpha \frac{\omega_{p\alpha}^2}{n_\alpha \omega^2} \int \frac{k_l p_{\alpha i} p_{\alpha j}\, \partial f_{0\alpha}/\partial p_{\alpha l} d^3\vec{p}_\alpha}{\gamma_\alpha^* [m_\alpha \gamma_\alpha^* (\omega + i\nu_\alpha) - \vec{k}\cdot\vec{p}_\alpha]}. \tag{5}$$

Here $\gamma_\alpha^* = (1 + \vec{P}_\alpha^2/m^2c^2)^{1/2}$ is the Lorentz factor and $\omega_\alpha = (4\pi n_\alpha e^2/m)^{1/2}$ is the α-type electron plasma frequency, respectively.

In order to take into consideration of the thermal effect consistently and obtain analytical results, we use the simplified relativistic Maxwellian distribution [31] instead of the relativistic water bag distribution or the drifting Jüttner distribution [32] for the beam electrons;

$$f_{0b} = \frac{n_b}{2\pi m \gamma_b^2 (T_{tb} T_{lb}^*)^{1/2}} e^{-P_x^2/2m\gamma_b T_{tb}} e^{-(P_z - P_{db})^2/2m\gamma_b^3 T_{lb}^*}, \tag{6}$$

where the Lorentz factor $\gamma_b = (1 + P_{db}^2/m^2c^2)^{1/2}$ and T_{tb}, T_{lb}^*, and P_{db} correspond to transverse thermal temperature, longitudinal thermal temperature, and drift momentum of the beam electrons, respectively. For convenience we denote $T_{lb} = \gamma_b^2 T_{lb}^*$. Since Eq. (6) is only the first-order approximation to the Jüttner distribution, it is only applicable for small momentum spread case. In the limit of $c \to \infty$, Eq. (6) can be simplified to the nonrelativistic drifting Maxwellian distribution. In the present calculation, the dense background electron component is approximately treated nonrelativistically.

As for the collision frequency, we take into account both intrabeam and interbeam collisions [33], where we have $\nu_b = \nu_{bb} + \nu_{bp} + \nu_{bi}$ for the beam electrons and $\nu_p = \nu_{pp} + \nu_{pb} + \nu_{pi}$ for the background electrons. The relativistic Coulomb logarithm [34] is used for beam electron-bulk plasma collision [35]. Moreover, we use an average temperature $\bar{T}_p = (T_{tp} + T_{lp} + T_{dp})/2$ to replace the isotropic thermal temperature T_α for the interspecies particle collisions to include the drifting effect. For intraspecies particle collisions, we still use the classical definition of the isotropic temperature [36]. Although the beam electron collision frequency is usually several orders smaller than the instability growth rate for a relativistic beam, we still include it here for a complete discussion.

For the CFI we assume the perturbation wave vector is in the $\hat{e}_x$ direction with the electromagnetic components $\vec{E}_{EM} = E_z \hat{e}_z$ and $\vec{B}_{EM} = B_y \hat{e}_y$. Under such assumptions, the space-charge effect [22] is neglected and the dispersion relation for the CFI can be obtained following Eq. (4):

$$\omega^2 \varepsilon_{zz} - k_x^2 c^2 = 0. \tag{7}$$

The TSI branch can be obtained similarly if we assume the perturbation is in the $\hat{e}_z$ direction with an electrostatic component $\vec{E}_{ES} = E_z \hat{e}_z$:

$$\varepsilon_{zz} = 0. \tag{8}$$

III. GROWTH RATES OF THE INSTABILITIES

A. Collisional current-filamentation instability

In this section we study the collisional effects on the CFI. Substitute Eq. (5) into Eq. (7), one can approximately get

$$\omega^2 - \sum_\alpha \frac{\omega_\alpha^2}{\gamma_\alpha^3} - c^2k_x^2 - \sum_\alpha \frac{\omega_\alpha^2}{\gamma_\alpha}\frac{v_{d\alpha}^2 + v_{l\alpha}^2}{2v_{t\alpha}^2}Z'_\alpha - i\sum_\alpha \frac{\omega_\alpha^2}{\gamma_\alpha^3}\frac{\nu_\alpha}{\sqrt{2}k_x v_{t\alpha}}Z_\alpha = 0, \quad (9)$$

where $Z_\alpha(\xi_\alpha)=\frac{1}{\sqrt{\pi}}\int_{-\infty}^{\infty}dt\frac{e^{-t^2}}{t-\xi_\alpha}$ is the plasma dispersion function [37], $\xi_\alpha=\frac{\omega+i\nu_\alpha}{\sqrt{2}k_x v_{t\alpha}}$, $v_{t\alpha}=\sqrt{T_{t\alpha}/\gamma_\alpha m}$, $v_{l\alpha}=\sqrt{T_{l\alpha}/\gamma_\alpha m}$, and $v_{d\alpha}=P_{d\alpha}/\gamma_\alpha m$. The number of primes on Z_α denotes the differentiation order. In the present paper, we mainly focus on a cold dense nonrelativistic plasma, thus we approximately have $\gamma_p=1$. From Eq. (9) one can see that quite similar to the nonrelativistic case [10], the classical anisotropic term v_{lb}^2/v_{tb}^2 driving the classical Weibel instability [38] is replaced by the drift-anisotropic term $(v_{lb}^2+v_{db}^2)/v_{tb}^2$. Thus, the CFI is still determined by the combination of the drift anisotropy of the beam and the background plasma in the relativistic case. In fact, Eq. (9) is formally the same as the nonrelativistic Eq. (18) in Ref. [10], thus the analytic solutions we obtained previously can be applied in the present paper if only the beam electron related terms be defined in the present relativistic way. Unlike the previous study [17,19,39], the CFI cannot be stabilized only by enhancing the beam thermal temperature under our relativistical model (6) even in the collisionless case. In the collisional case, one can see that collisional effects appear in the fourth and the fifth terms on the left-hand side (LHS) of Eq. (9). The one in the fourth term denotes the collisional effects in the direction parallel to the wave vector, which mainly results in detuning between the particle density perturbations and the reactive fields and then attenuates the CFI. The one in the fifth term denotes the collisional effects in the direction perpendicular to the wave vector, which mainly interferes with the collective movements of the plasmas and leads to enhancement of the CFI. Next we mainly focus on the numerical solution of Eq. (9) and apply our theory to the physical process relevant to FIS.

In our previous study [10], we have used the power series and the asymptotic series expansions for the plasma dispersion function. The beam-plasma system was divided into three cases: the kinetic domain, the hydrodynamic domain, and the hybrid domain which correspond to $|\xi_{b,p}| \ll 1$, $|\xi_{b,p}| \gg 1$, and $|\xi_b| \ll 1$, $|\xi_p| \gg 1$, respectively. Since the thermal pressure is rather strong in the kinetic region, here we still follow our previous method for the convenience of discussion. Although we have artificially divided the plasmas into three catalogs, the numerical calculations of the dispersion relation [Eq. (9)] using the Padé approximation of the plasma dispersion function [25] indeed include regions $|\xi_\alpha| \sim 1$, where the thermal effect is significant, too.

Figure 1 shows the linear CFI growth rates at some typical bulk plasma densities. From Fig. 1(a) one finds that the CFI is mainly suppressed by collisional effects at a lower bulk plasma density. As the density becomes larger, collisional effects turn to enhance the CFI, and the increment can be up to two orders for an extremely high density. This is demonstrated more clearly in Figs. 2(a) and 2(c), where the collisional effects on the maximal CFI growth rate are depicted for bulk temperatures 250 and 1000 eV, correspondingly. We have argued in the nonrelativistic case that collisional effects tend to attenuate the CFI for symmetric (where $n_b=n_p$) or quasisymmetric counterstreaming while enhance it for extremely asymmetric counterstreaming (where $n_p \gg n_b$). Here we find the similar results in the relativistic case. This can be understood as follows. Usually, random collisions have two effects on the CFI. First, the collisions parallel to the wave vector change ω to $\omega+i\nu_\alpha$, resulting in detuning between the particle perturbations and their corresponding reactive fields. This cancels the growth rate in the order of ν_α. Second, the collisions perpendicular to the wave vector can interfere with the collective movement of the dense bulk plasma, which can reduce the stabilization effect of the background to the beam-plasma system. This can lead to enhancement of the CFI especially when the background plasma is much denser than the beam. The collisional effect can only be significant if it gets over the thermal effect, where it shifts the plasma from kinetic region to hydrodynamic region.

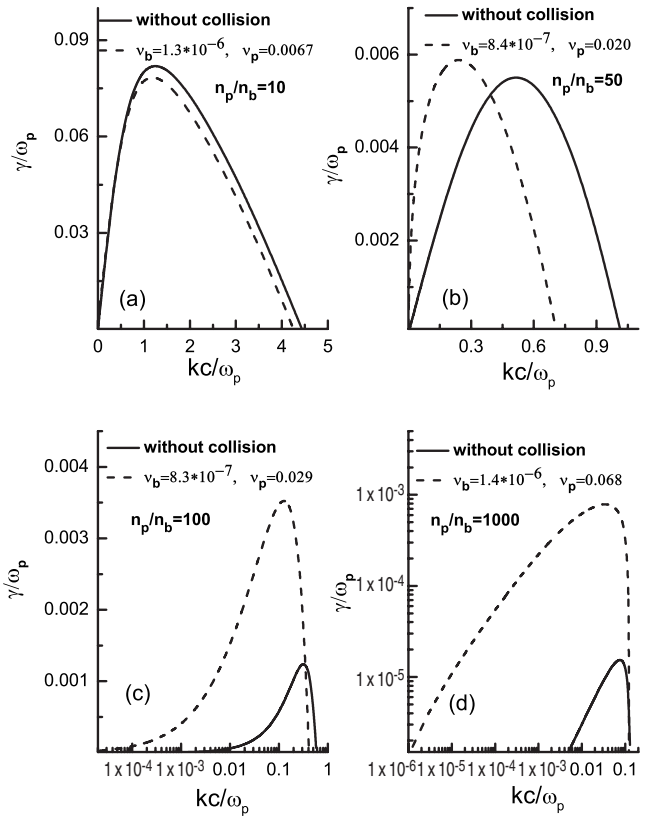

FIG. 1. The typical linear growth rate of the CFI versus the wave number k obtained by solving Eq. (9). The growth rate and the collision frequency are normalized to the bulk plasma frequency. The parameters are $n_b=10^{21}$ cm^{-3}, $\gamma_b=2.93$, $T_{tb}=T_{lb}=30$ keV, and $T_{tp}=T_{lp}=250$ eV.

For symmetric or quasisymmetric counterstreaming shown in Figs. 1 and 2, the attenuation effects excess the

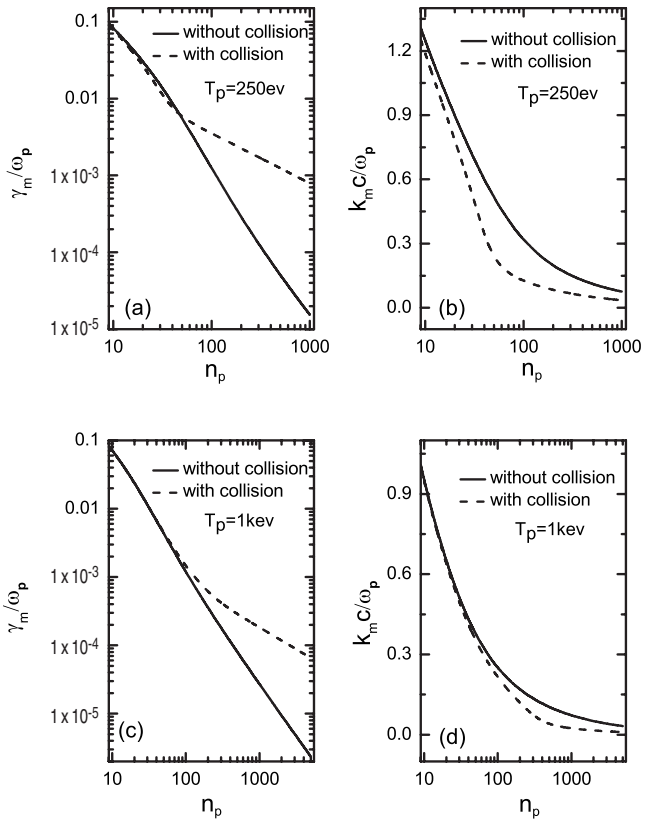

FIG. 2. [(a) and (c)] The largest linear growth rate and [(b) and (d)] the corresponding wave number of the CFI versus the bulk density n_p obtained by solving Eq. (9). The parameters are the same as those in Fig. 1.

enhancing effects, resulting in reduction in the CFI growth rate. For extremely asymmetric counterstreaming, the drifting velocity of the bulk plasma $v_{dp}=-v_{db}n_b/n_p$ is rather small so that the drift anisotropy of the background plasma contributes little to the filamentation instability of the beam-plasma system. Therefore, the CFI of the beam-plasma system is mainly driven by the beam drift anisotropy. The dense background, however, usually stabilizes it as shown by the solid line in Figs. 2(a) and 2(c), where we can see that the CFI is reduced as the bulk gets denser. When collisions are taken into account, the beam electron collision frequency, which is at least three orders smaller than the largest CFI growth rate in the case close to FIS (see Fig. 1), can hardly decrease the CFI. As for the bulk electron collision frequency, it can be much larger than the CFI growth rate so that it causes nearly complete detuning between the background electron perturbations and their corresponding reactive fields, resulting in reduction in the contribution of the background electron to the beam-plasma CFI. However, since the bulk electron contributes little to the CFI, the reduction which the bulk electron collision makes to the CFI is small. Instead, the random bulk electron collision interferes with the ordered collective movement of the bulk electrons and greatly decreases the stabilization effect of the background to the beam-plasma system, which is shown by the last term on the LHS of Eq. (9), leading to the increment of the CFI. Moreover, the bulk collision changes $|i\omega| \ll k_x v_{tp}$ to $|i\omega+\nu_p| \gg k_x v_{tp}$ and shifts the bulk plasma from the kinetic domain to the hydrodynamic domain, resulting in the reduction in the thermal stabilization effect and thus resulting in increment of the CFI, too. For the extremely asymmetric counterstreaming shown in Figs. 1 and 2, the collisional enhancing effects excess the attenuating effects, so the growth rate, especially the maximum growth rate of the filamentation mode, is increased finally. For short-wavelength regions where $|\omega+i\nu_\alpha| < kv_{t\alpha}$, the beam-plasma system is in the kinetic domain, and the thermal effect is rather significant. It is seen from Fig. 1 that the CFI is still attenuated in these regions.

Since the CFI is enhanced in the dense core region instead of being stabilized, it suggests that the original fast electron beam may potentially break into small filaments even in the dense region at the linear stage. As one can see from Fig. 1(d), the growth rate is nearly three orders higher than the beam collision frequency for the $T_p=250$ eV case. It indicates that filamentation induced kinetic anomalous target heating [2,5] might be dominant in the previous cone guided FIS experiment [21]. For the $T_p=1$ kev case, the CFI growth rate is still one order higher than the fast electron collision frequency in the dense region $n_p/n_b=5000$. Although the real beam electron temperature might be a little higher than our present assumption, the CFI growth rate is estimated to be at least in the same order as the beam electron collision frequency. Thus the CFI is still very important for the real FIS target heating. Meanwhile, we can see from Fig. 1 and Figs. 2(b) and 2(d) that the most unstable filamentation mode which shapes the electron beam most is shifted to the long-wavelength region as the bulk density becomes larger. The shift is more significant when collisional effects are taken into consideration. Thus, collisional effects can result in much bigger filaments. As the density ratio of the bulk to the beam gets over 100, the wavelength of the most unstable mode gets over $10c/\omega_p$, which is estimated to be in the order of 1 μm. Since it is still much smaller than the electron-beam radius generated by today's laser, our assumption of an infinite plasma is reasonable. However, it may add more difficulty to particle-in-cell simulations because larger area is needed to exclude the boundary condition [24] effect. This is an important problem which needs further study.

B. Collisional two-stream instability

Although there have been some analytical studies [11,27], generally it is very difficult to get analytic solutions for collisional TSI, especially for parameters close to FIS where the dispersion function cannot simply be expanded in series. Therefore in this subsection we mainly focus on the numerical solutions of the dispersion equation via the bulk density. Emphasis is laid on the different roles the collisional effects play to the CFI and the TSI.

Substitute Eq. (5) into Eq. (8), we can obtain

$$1-\frac{\omega_b^2}{\gamma_b^3}\frac{\omega+i\nu_b}{\omega}\left(\frac{Z'(\zeta_b)}{2k_z^2v_{lb}^2}-1.5\beta_b\frac{Z''(\zeta_b)}{\sqrt{2}k_z^2v_{lb}c}\right)-\omega_p^2\frac{\omega+i\nu_p}{\omega}\frac{Z'(\zeta_p)}{2k_z^2v_{lp}^2}=0, \tag{10}$$

where $\zeta_\alpha=(\omega-k_zv_{d\alpha}+i\nu_\alpha)/(\sqrt{2}k_xv_{l\alpha})$ and $\beta_b=P_{db}/\gamma_b mc$. For

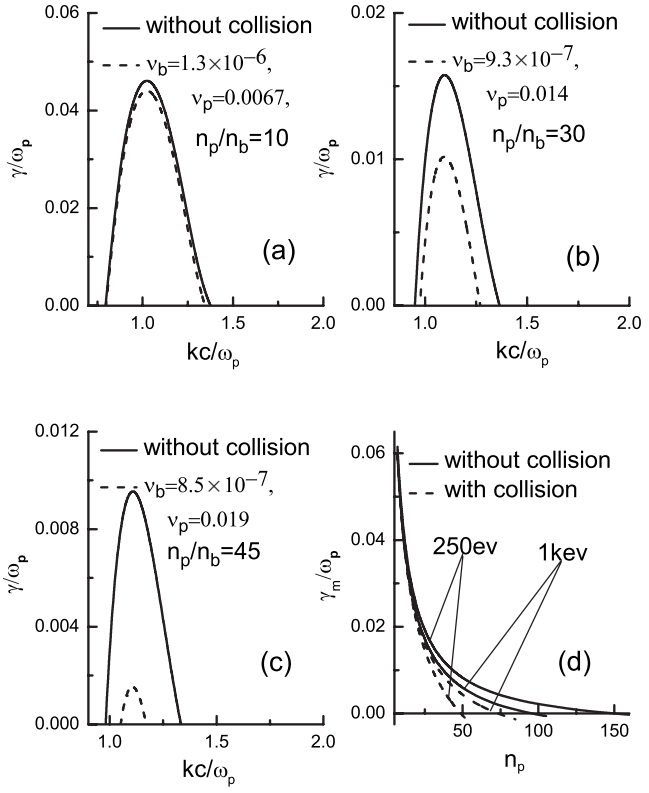

FIG. 3. [(a)–(c)] The typical linear growth rate of the TSI versus the wave number k and (d) the largest growth rate versus the bulk density n_p obtained by solving Eq. (10). The parameters are the same as those in Fig. 1.

TSI the collisions in Eq. (10) are in the direction parallel to the wave vector.

Different from the electromagnetic filamentation instability, the TSI is electrostatic and is driven by the inverse Landau damping the beam electron undergoes. Since collisional effect can destroy the resonance between the particle and the reactive fields, it can decrease the inverse Landau damping process, resulting in reduction in the TSI. However, usually ν_b is much smaller than the TSI growth rate, it can hardly attenuate the TSI. Instead, the attenuation is mainly caused by the bulk electron collision. The random bulk collision interferes with the collective oscillation of the bulk electron and further the organized space-charge separation, which leads to suppression of the electrostatic field. If the collision frequency is large enough, it will finally stabilize the TSI. Figure 3 shows the linear growth rate of the TSI under parameters close to the fast ignition, where the most accurate Padé approximation Z_{53} to the plasma dispersion function given in Ref. [25] is also used. From Figs. 3(a)–3(c) we can see that both the growth rate and the unstable range are suppressed. As the bulk density becomes larger, the suppression becomes more significant. Figure 3(d) shows the collisional effects on the most unstable two-stream mode. It is seen that the most unstable mode is always attenuated and finally stabilized when the bulk plasma reaches the solid density, which is in agreement with the simulation of Kemp *et al.* [7] It is interesting to mention that the collision in the direction parallel to the wave vector attenuates the corresponding instability both in the CFI and the TSI cases although the underlying physical mechanisms are different. Notice that the shift made by the collisional effects to the most unstable two-stream mode in the k space is small and can be neglected. For real FIS the beam temperature might be a little higher than our present case. The TSI would even be stabilized in lower density regions. Therefore, the TSI is not as important as the CFI in the FIS.

IV. SUMMARY

We have investigated theoretically the collisional effects on the relativistic CFI and the TSI. The different roles collisions play on the CFI and the TSI are identified. The theory is then applied to the beam and plasma parameter regimes where both the collisional effects and the kinetic collective instability are important in the FIS. Since we use a simplified relativistic drifting Maxwellian distribution, our theory applies to a low-temperature relativistic beam.

We show that the CFI is first attenuated by the collisional effects when the bulk plasma density is not so large. As the density ratio of the bulk plasma to the beam gets larger than 50, collisional effects turn to enhance the CFI, and the increment can be 2 orders of magnitude larger than the collisionless case in the dense core region. Contrarily, the TSI is always attenuated by the collisions and finally stabilized when the bulk plasma reaches the solid density. Furthermore, collisional effects shift the most unstable filamentation mode to the long-wavelength region and result in bigger filaments. The present investigation indicates that the incoming fast electron beam inclines to break into small filaments even in the dense region. It also indicates that the anomalous kinetic target core heating potentially exists and might be important for the fast ignition scenario.

ACKNOWLEDGMENTS

This work was supported by the National Nature Science Foundation of China (Grants No. 10425416, No. 60621063, No. 10734130, and No. 10828509), the National High-Tech ICF Committee, and National Basic Research Program of China (Grants No. 2007CB815101 and No. 2007CB815105). C.R. was supported by (U.S.) Department of Energy under Grants No. DE-FG02-06ER54879 and No. DE-FC02-04ER54789.

[1] A. Pukhov and J. Meyer-ter-Vehn, Phys. Rev. Lett. **79**, 2686 (1997).
[2] M. Honda, J. Meyer-ter-Vehn, and A. Pukhov, Phys. Rev. Lett. **85**, 2128 (2000).
[3] J. T. Mendonca, P. Norreys, R. Bingham, and J. R. Davies, Phys. Rev. Lett. **94**, 245002 (2005).
[4] R. J. Mason, Phys. Rev. Lett. **96**, 035001 (2006).
[5] Y. Sentoku, K. Mima, P. Kaw, and K. Nishikawa, Phys. Rev. Lett. **90**, 155001 (2003).
[6] R. B. Campbell, R. Kodama, T. A. Mehlhorn, K. A. Tanaka, and D. R. Welch, Phys. Rev. Lett. **94**, 055001 (2005).
[7] A. J. Kemp, Y. Sentoku, V. Sotnikov, and S. C. Wilks, Phys. Rev. Lett. **97**, 235001 (2006).
[8] B. Chrisman, Y. Sentoku, and J. Kemp, Phys. Plasmas **15**, 056309 (2008).
[9] M. Honda, Phys. Rev. E **69**, 016401 (2004).
[10] B. Hao, Z.-M. Sheng, and J. Zhang, Phys. Plasmas **15**, 082112 (2008).
[11] L. A. Cottrill, A. B. Langdon, B. F. Lansinski, S. M. Lund, K. Molvig, M. Tabak, R. P. J. Town, and E. A. Williams, Phys. Plasmas **15**, 082108 (2008).
[12] Y. Sentoku, K. Mima, S. Kojima, and H. Ruhl, Phys. Plasmas **7**, 689 (2000).
[13] M. Tabak, J. Hammer, M. E. Glinsky, W. L. Kruer, S. C. Wilks, J. Woodworth, E. M. Campbell, M. D. Perry, and R. J. Mason, Phys. Plasmas **1**, 1626 (1994).
[14] S. A. Bludman, K. M. Watson, and M. N. Rosenbluth, Phys. Fluids **3**, 747 (1960).
[15] A. Bret, M. C. Firpo, and C. Deutsch, Phys. Rev. E **70**, 046401 (2004).
[16] B. Hao, Z.-M. Sheng, C. Ren, and J. Zhang (unpublished).
[17] K. Molvig, Phys. Rev. Lett. **35**, 1504 (1975).
[18] T. Okada and K. Niu, J. Plasma Phys. **24**, 483 (1980).
[19] A. Karmakar and Ph. D. Thesis, *Theory and Simulations of Nonlinear and Inelastic Processes Laser Plasma Interactions* (Heinrich-Heine University, Dusseldorf, Germany, 2008).
[20] J. M. Wallace, J. U. Brackbill, C. W. Cranfill, D. W. Forslund, and R. J. Mason, Phys. Fluids **30**, 1085 (1987).
[21] R. Kodama, P. A. Norreys, K. Mima, A. E. Dangor, R. G. Evans, H. Fujita, Y. Kitagawa, K. Krushelnick, T. Miyakoshi, N. Miyanaga, T. Norimatsu, S. J. Rose, T. Shozaki, K. Shigemori, A. Sunahara, M. Tampo, K. A. Tanakaka, Y. Toyama, T. Yamanaka, and M. Zepf, Nature (London) **412**, 798 (2001).
[22] M. Tzoufras, C. Ren, F. S. Tsung, J. W. Tonge, W. B. Mori, M. Fiore, R. A. Fonseca, and L. O. Silva, Phys. Rev. Lett. **96**, 105002 (2006).
[23] M. Honda, J. Meyer-ter-Vehn, and A. Pukhov, Phys. Plasmas **7**, 1302 (2000).
[24] C. Ren, M. Tzoufras, F. S. Tsung, W. B. Mori, S. Amorini, R. A. Fonseca, L. O. Silva, J. C. Adam, and A. Heron, Phys. Rev. Lett. **93**, 185004 (2004).
[25] P. Martín, G. Donoso, and J. Z. Cristi, J. Math. Phys. **21**, 280 (1980).
[26] L. Landau, J. Phys. (USSR) **10**, 25 (1946).
[27] H. E. Singhaus, Phys. Fluids **7**, 1534 (1964).
[28] P. L. Bhatnagar, E. P. Gross, and M. Krook, Phys. Rev. **94**, 511 (1954).
[29] H. Lee and L. E. Thode, Phys. Fluids **26**, 2707 (1983).
[30] A. R. Bell, J. R. Davies, S. Guerin, and H. Ruhl, Plasma Phys. Controlled Fusion **39**, 653 (1997).
[31] K. M. Watson, S. A. Bludman, and M. N. Rosenbluth, Phys. Fluids **3**, 741 (1960).
[32] T. P. Wright and G. R. Hadley, Phys. Rev. A **12**, 686 (1975).
[33] C. Deutsch, A. Bret, M. C. Firpo, and P. Fromy, Phys. Rev. E **72**, 026402 (2005).
[34] A. A. Solodov and R. Betti, Phys. Plasmas **15**, 042707 (2008).
[35] J. D. Huba, *NRL Plasma Formulary* (Naval Research Laboratory, Washington, DC, 2004), p. 33.
[36] V. P. Krainov, J. Phys. B **36**, 3187 (2003).
[37] B. D. Fried, C. L. Hedrick, and J. McCune, Phys. Fluids **11**, 249 (1968).
[38] E. S. Weibel, Phys. Rev. Lett. **2**, 83 (1959).
[39] L. O. Silva, R. A. Fonseca, J. W. Tonge, W. B. Mori, and J. M. Dawson, Phys. Plasmas **9**, 2458 (2002).